

A design for preparation of textured piezoelectric ceramics based on the phase-field simulation

Yongmei Zhang* and Liangliang Liu†,‡

*College of Information Science and Engineering, Shanxi Agricultural University
Jinzhong 030801, P. R. China

†College of Materials Science and Engineering, Taiyuan University of Technology
Taiyuan 030024, P. R. China

‡liuliangliang@tyut.edu.cn

Received 1 August 2022; Revised 16 August 2022; Accepted 19 August 2022; Published 14 September 2022

To solve the problem of directional arrangement of small template particles, we designed a lamination technique for the preparation of dense ceramics with high texture degree based on the phase-field simulation. Referring to the experimental data, the initial microstructures of the template and matrix layers were constructed. The effect of the average length of template on the coarsening behavior of the template layer was investigated in detail. The results suggested that there was a stable stage in the growth process of template grains, which would be conducive to the densification of textured ceramics. This phenomenon has been confirmed by corresponding experiments. In addition, we demonstrated a critical thickness of matrix layer for the preparation of highly textured ceramics by using the template with various average lengths. The grain size of highly textured ceramics could be controlled by adjusting the template size and thickness of matrix layer.

Keywords: Design; phase-field simulation; textured ceramics; grain growth.

1. Introduction

As is known to all, the texturing technique can improve the piezoelectric properties of ceramics by regulating microstructure and grain orientation, and textured piezoelectric ceramics exhibit highly anisotropic features similar to single crystal.^{1,2} Up to now, various textured piezoelectric ceramics have been successfully synthesized by the (reaction) templated grain growth, which has been proved to be an effective and inexpensive method.^{3–11} These studies have confirmed that texture degree was directly proportional to the electrical properties of the textured ceramics. To obtain high texture degree, templates need to be selected in larger size because it is easy to complete the parallel arrangement in matrix. However, the usage of large particles is not only conducive to the densification of ceramics, but is also easy to induce abnormal grain growth (AGG) during sintering.^{12–15} In addition, templates were synthesized by molten salt method, and their compositions generally deviated from the stoichiometric ratio.^{16–21} Thus, in order to further improve the electrical properties of textured ceramics, the size and content of templates should be as small as possible, especially when heterogeneous templates are used. For this case, the conventional preparation process was difficult to synthesize dense piezoelectric ceramics with high texture degree.

Recently, we found that the short needle-like particles could be easily arranged into tape along the casting direction when the microcrystals synthesized by the molten salt method

were used as raw materials. Our simulation and experimental results confirmed that the competitive growth of microcrystalline particles effectively inhibited the AGG, resulting in the preparation of dense ceramics with high texture degree.^{10,22,23} Inspired from the above considerations, we proposed a novel strategy to simultaneously achieve high texture degree and density of piezoelectric ceramics under the condition of low template content. As shown in Fig. 1, the layers of matrix and template were formed by tape casting, respectively. Then, the template and matrix layers were pressed into a green body in a certain proportion. In this process, the effects of two important parameters, template size and matrix layer thickness, needed to be investigated, which was hard to be revealed by the experimental method. With the development of computer technology, simulation has become an important means to study the grain growth behavior of polycrystalline materials. The phase-field model was considered to have remarkable advances because grain boundary position was not required for continuous tracking.^{24,25} In our previous work, a phase-field model modified by introducing grain boundary energy anisotropy was developed to describe the evolution of texture microstructure.^{22,23} Thus, a design for preparation of textured piezoelectric ceramics is expected by the phase-field simulation.

The aim of our work is to investigate the effects of template size and matrix layer thickness on the grain growth behaviors. It will provide a reliable basis for the preparation of dense piezoelectric ceramics with high texture degree.

‡Corresponding author.

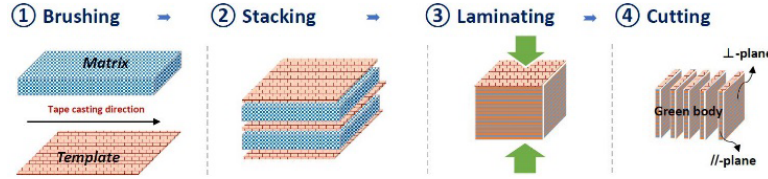


Fig. 1. Schematic illustrations showing the preparation process of textured ceramics.

2. Experimental Method

The phase-field model followed that of Chen.²⁴ The time-dependent Ginzburg–Landau equation for the long-range order could be expressed as follows:

$$\frac{d\eta_i(\mathbf{r},t)}{dt} = -L_i \frac{\delta F}{\delta \eta_i(\mathbf{r},t)}, \quad (1)$$

where L_i is the mobility of the grain boundary migration. The system free energy F can be expressed as follows:

$$F = F_0 + \int \left[\sum_{i=1}^q \left[-\frac{\eta_i^2}{2} + \frac{\eta_i^4}{4} \right] + \sum_{i=1}^q \sum_{j>1}^q \eta_i^2 \eta_j^2 + \sum_{i=1}^q \frac{K}{2} (\nabla \eta_i(\mathbf{r}))^2 \right] d^3r, \quad (2)$$

where K denotes the gradient energy coefficient. In this work, the tetragonal tungsten bronze structured $\text{KSr}_2\text{Nb}_5\text{O}_{15}$ (KSN) was used as a reference object. According to the experimental results, the K value was different for the template grains in different directions, which was considered to be the same for the matrix grains.^{10,22} For simplicity, an anisotropic parameter was introduced and K was discretized in rectangular coordinate system

$$k_{\perp} = Ck_{\parallel}, \quad (3)$$

$$\frac{k_{\parallel}^2 + k_{\perp}^2}{2} = K^2, \quad (4)$$

where k_{\parallel} and k_{\perp} are the gradient energy coefficients along the vertical and parallel tape casting direction, respectively. The lattice in the calculation was sampled into $N \times M$ grid points; periodic boundary conditions were applied. The following values were assigned to the parameters in the phase-field equation: $K = 2.0$, $L_i = 1.0$, $q = 400$, $\Delta t = 0.1$, $\Delta x = 2$. $C = 1$ for the matrix and 20 for the template. The time scale was represented by the time step (TS). TS = 1 corresponds to one Δt . In order to show the microstructural evolution, we defined a function $\varphi(\mathbf{r})$

$$\varphi(\mathbf{r}) = \sum_{i=1}^q \eta_i^2(\mathbf{r}). \quad (5)$$

The values of $\varphi(\mathbf{r})$ were shown as color images.

KSN matrix and template were fabricated by a solid-state reaction route and molten salt synthesis. 6 mol.% Bi_2O_3 was

added as sinter aid. At first, matrix and template layers were prepared by the brushing technique, respectively.¹⁰ Then, the matrix and template layers were laminated together at 70°C and 100 MPa for 15 min. The binder and plasticizer were removed by heating samples at 0.4°C/min to 600°C for 4 h. The samples were presintered at 1200°C for 2 h prior to the sintering at 1300°C for 2 h, e.g., two-step sintering technique. The density was measured by the Archimedes method with the bulk samples. X-ray diffraction (XRD) analysis (Panalytical X'Pert PRO, Holland) and scanning electron microscopy (SEM) observation (Tescan VEGA3 and Quanta 600 FEG, respectively) were used to study texture quality and grain morphologies.

3. Results and Discussion

According to the KSN particle size, the initial microstructures were set. As shown in Fig. 2, the particles prepared by solid-state reaction route had irregular morphology and diameter of about 1 μm . The needle-like particles fabricated by molten salt synthesis had uniform diameters of 1 μm . The length of these particles could be freely regulated by the ball milling process.¹⁵ We considered the matrix particle as a circle and four grid points were equal to 1 μm . Thus, the initial microstructure of matrix and template layer could be set by filling in the mesh with circles ($r = 2$ grid points) and rectangles (the width of four grid points). The thickness of the template layer was set to 20 grid points because the thinnest single layer we could form was 5 μm at present. The formation of the initial microstructure was described in detail in the previous report.^{22,23} In this work, different average lengths of template (12–28 grid points, denoted hereafter as LT = 12, 16, 20, 24, and 28) were set. The following normal distribution function was used to set the radius of the initial particle:

$$f(x) = \frac{1}{\sigma\sqrt{2\pi}} \exp\left(-\frac{(x-\mu)^2}{2\sigma^2}\right), \quad (6)$$

where $\mu = \text{LT}$, $\sigma = \frac{10}{3}$.

The effect of template length on the grain growth behaviors was investigated at first. One template layer was added in the 120×300 system for all cases. Figure 3 shows the microstructure evolutions for the cases of LT = 12 and 28. It can be observed that some matrix grains far away from the template gradually grew with the increase of TS. The matrix grains adjacent to the template grains were quickly absorbed.

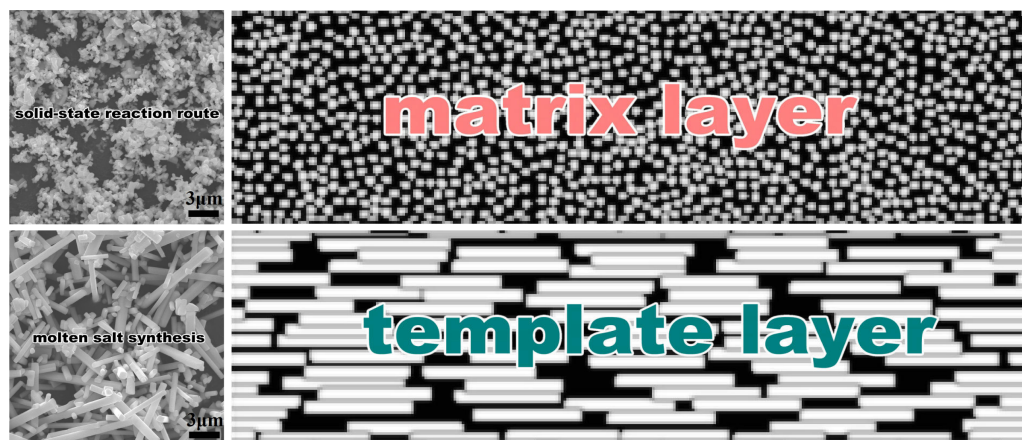


Fig. 2. SEM images of the KSN particles and initial microstructures of matrix and template layer.

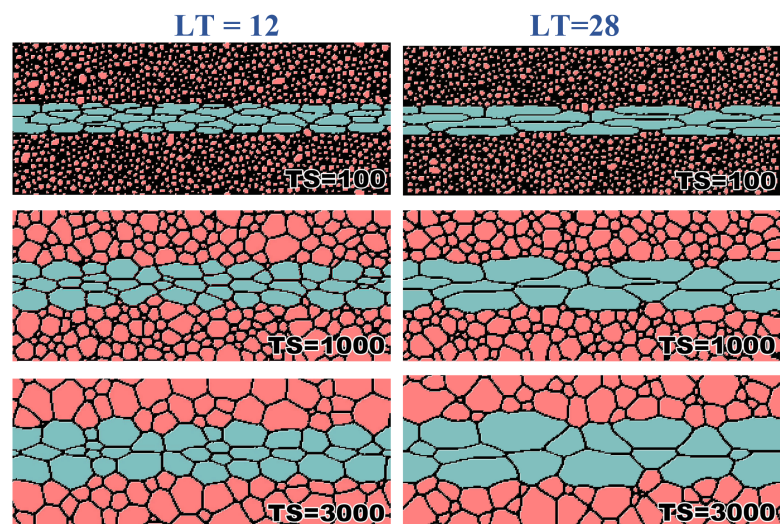


Fig. 3. Microstructure evolutions of LT = 12 and 28 at different TSs.

The comparison of the two cases of LT = 12 and 28 showed that there was almost no difference in the matrix grain microstructures. This means that the length of template in the layer had little influence on the growth behavior of matrix grain. However, the size and shape of the template grains changed significantly. It was found that the template grains grew mainly along the vertical direction by absorbing the surrounding small matrix grains, but not in the parallel direction because they touched each other. Compared with the outer grains, the inner grains of the template layer slowly shrank because they did not have the advantage of size.²² Obviously, this process effectively limited the rapid growth of large template grains. As seen in Fig. 3, the size of some matrix grains exceeded that of template grains for the case of LT = 12 at TS = 3000. However, with the increase of template length, the size advantage of template grains could be maintained for a longer time. In addition, it can be seen that the morphology of template grains kept the larger aspect ratio with the increase of TS for the case of LT = 28.

To investigate the kinetics of template grain growth, we selected the template grains in contact with matrix grains to study their evolution process. Figure 4 shows the changes in the average area of all grains and the template grains in contact with matrix grains as a function of the TS. The growth curves of all grains were shown as a straight line. This was because the number of matrix grains was much larger than that of template grains. As shown in Fig. 4, the growth process of template grains could be divided into three stages for the case of LT = 12: rapid growth (TS < 500), steady growth (TS = 500–2500), and stop growing (TS > 3000). According to the analysis in Fig. 3, this could be attributed to the result of the competitive growth of template and matrix grains. In fact, the stage of rapid growth was the same as the conventional process, which belonged to the AGG process.^{12–14} The second stage was linear shape, indicating the phenomenon of normal grain growth (NGG). What's exciting was that the first stage was very short and the second stage covered a wide time range. This feature suggested that this design was feasible

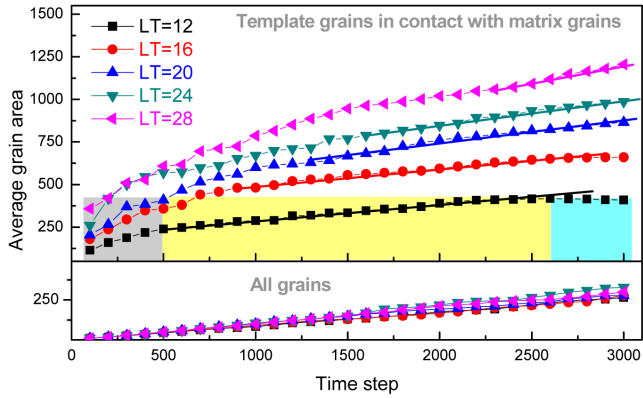


Fig. 4. Changes in the average area of all grains and the template grains in contact with matrix grains as a function of the TS.

and expected to guide the preparation of dense ceramics with high texture degree. It was found that the duration of the rapid growth would be widened as the template length increased. This suggested that the use of long template particles was unfavorable to the densification process of textured ceramics.

To achieve a higher texture with a lower template volume fraction, the effect of the matrix layer thickness on the microstructure evolution was investigated. Figure 5 shows the microstructure evolutions of $LT = 12$ for the different thicknesses of matrix layer ($x = 20$ and 30 grid points). When the matrix layer was thin ($x = 20$ grid points), the template grains grew rapidly to impinge onto each other at $TS = 2000$. This simulation result agreed with experimental results that a shorter average distance and high-volume fraction of templates lead to faster texture development.^{26–28} When the thickness of the matrix layer increased to 30 grid points, some matrix grains had enough time to grow and their size even exceeded that of the adjacent template grains. So, it was almost impossible to observe the matrix layer swallowed up

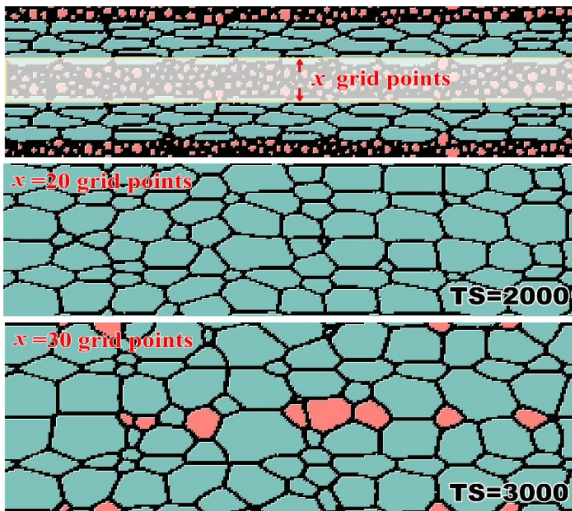


Fig. 5. Microstructure evolutions of $LT = 12$ for the different thickness of matrix layer ($x = 20$ and 30 grid points).

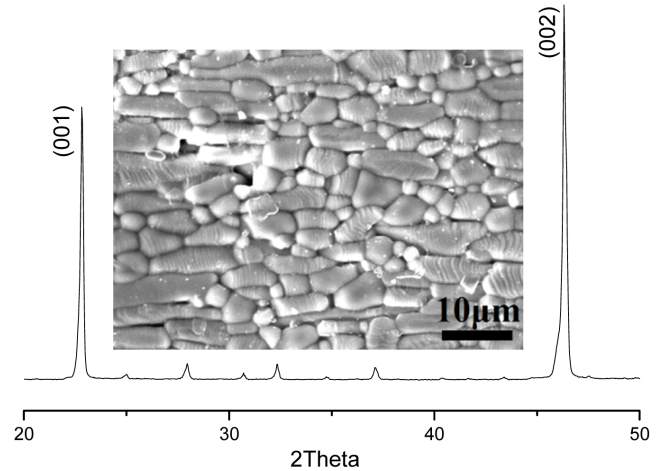


Fig. 6. XRD pattern and SEM image of the textured KSN ceramics prepared by a laminated process.

by the template layers. In the case of $x = 30$ grid points, the two template layers have been closed and a small amount of matrix grains remained. Although the residual matrix grains could disappear in theory, it took a very long time. Based on this, it was considered that the thickness could be optimized when the size of matrix grains was larger than that of adjacent template grains. According to the simulation results, we carried out the corresponding experiment using the KSN particles with an average length of $3 \mu\text{m}$ as raw material. The relative density of the textured KSN ceramics was up to 95%. Figure 6 shows the XRD pattern and SEM image of the textured KSN ceramics prepared by a laminated process. The experimental results indicated that dense ceramics with high texture were successfully prepared by the design method. As shown in Figs. 5 and 6, the simulation and experiment results regarding the grain shapes and microstructures are well agreed. This further confirmed that the preparation of textured ceramics with the target microstructure is feasible by the design method.

A series of simulations similar to those in Fig. 5 were systematically carried out with different average lengths of the template ($LT = 12, 16, 20, 24,$ and 28). The critical thickness of matrix layer could be obtained by increasing the distance between template layers as long as the content of matrix grains $\leq 10\%$. Figure 7 shows the relationship between the critical thickness of matrix layer and average length of the template, and simulated microstructures at the thickness of matrix layer. The critical thickness increased with the increase of the average length of the templates, but its increasing rate decreased gradually. This suggested that the matrix content could be increased with the increase of the average length of the template. As shown in the simulated microstructures (Fig. 7), a small number of matrix grains were observed for all of the cases, and some of these grains were larger than the surrounding template grains. It was worth noting that the template grains still maintained the strip morphology, and

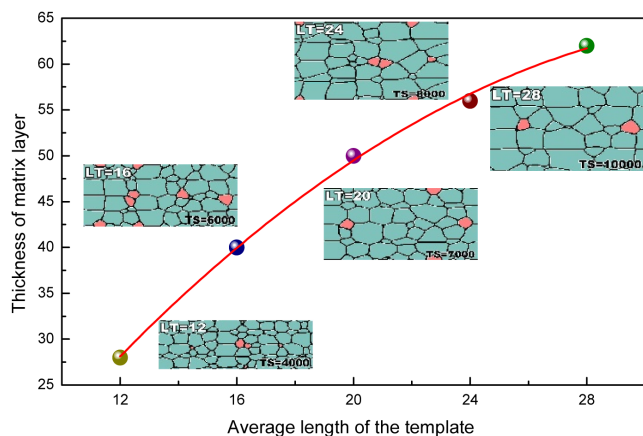


Fig. 7. Relationship between the critical thickness of matrix layer and average length of the template, and simulated microstructures at the thickness of matrix layer.

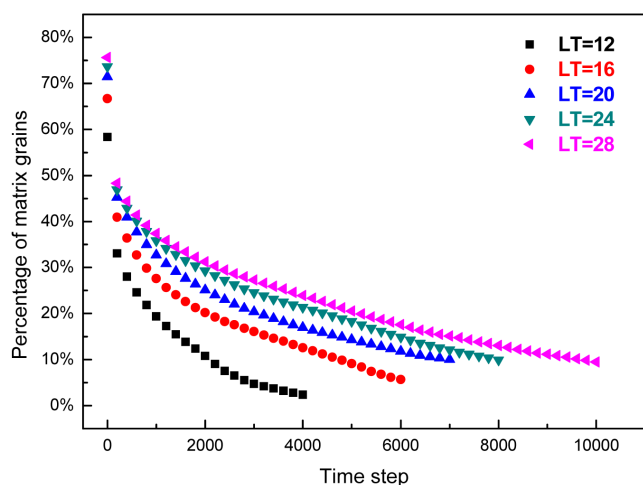


Fig. 8. Change in the percentage of matrix grains as a function of the TS under the critical thickness conditions.

their size increased evidently with the increase of LT. This implied that the grain size of textured ceramics could also be easily regulated by adjusting the average length of the template and matrix thickness. Figure 8 shows the change in the percentage of matrix grains as a function of the TS under the critical thickness conditions. It can be seen that the content of matrix grains decreased rapidly for the case of $LT = 12$. With the increase of LT, the decrease rate of matrix grain content become slower. When LT was increased to 28, the curve changed very slowly after $TS = 1000$. This means that a long holding time was necessary for the ceramics with high texture degree obtained by increasing the average length of the template.

4. Conclusions

A lamination technique was designed to fabricate the dense textured ceramics using needle-like particles as template.

Textured KSN ceramics was used as a target. The effect of the average template length on the grain growth behaviors and optimization of matrix layer thickness on the texture degree were investigated in detail. It was found that the length of template had little influence on the growth behavior of matrix grain. A phenomenon of template grain growth similar to NGG occurred in a wide range of time for all cases, which facilitated the densification of textured ceramics. The critical thickness increased with the increase of the average length of the templates, but its increasing rate decreased gradually. This study suggested that dense ceramics with a high texture degree could be obtained using the short particle as template by the lamination technique. Under the condition of high texture degree, the matrix content could be further increased with the increase of average template length. In addition, the grain microstructures of highly textured ceramics could be regulated by adjusting the template size and thickness of matrix layer. This design will be an important reference for the preparation of high-performance textured piezoelectric ceramics.

Acknowledgments

This work was supported by the National Natural Science Foundation of China (No. 52102138) and Fundamental Research Program of Shanxi Province (No. 202103021224080).

References

- G. L. Messing, S. Poterala, Y. Chang, T. Frueh, E. R. Kupp, B. H. Watson, R. L. Walton, M. J. Brova, A. K. Hofer, R. Bermejo and R. J. Meyer Jr., Texture-engineered ceramics — Property enhancements through crystallographic tailoring, *J. Mater. Res.* **32**, 3219–3241 (2018).
- B. Zhang, R. B. Sun, F. Wang, T. Feng, P. Zhang and H. Luo, Pyroelectric properties of $91.5\text{Na}_{0.5}\text{Bi}_{0.5}\text{TiO}_3-8.5\text{K}_{0.5}\text{Bi}_{0.5}\text{TiO}_3$ lead-free single crystal, *J. Adv. Dielect.* **11**, 2150023 (2021).
- Y. Yan, L. D. Geng, H. Liu, H. Leng, X. Li, Y. U. Wang and S. Priya, Near-ideal electromechanical coupling in textured piezoelectric ceramics, *Nat. Commun.* **13**, 3565 (2022).
- S. Yang, J. Li, Y. Liu, M. Wang, L. Qiao, X. Gao, Y. Chang, H. Du, Z. Xu, S. Zhang and F. Li, Textured ferroelectric ceramics with high electromechanical coupling factors over a broad temperature range, *Nat. Commun.* **12**, 1414 (2021).
- W.-S. Kang, T.-G. Lee, J.-H. Kang, J.-H. Lee, G. Choi, S.-W. Kim, S. Nahm and W. Jo, Bi-templated grain growth maximizing the effects of texture on piezoelectricity, *J. Eur. Ceram. Soc.* **41**, 2482 (2021).
- Y. Chang, J. Wu, B. Yang, H. Xie, S. Yang, Y. Sun, S. Zhang, F. Li and W. Cao, Large, thermally stabilized and fatigue-resistant piezoelectric strain response in textured relaxor-PbTiO₃ ferroelectric ceramics, *J. Mater. Chem. C* **9**, 2008 (2021).
- L. Wei, X. Chao, X. Han and Z. Yang, Structure and electrical properties of textured $\text{Sr}_{1.85}\text{Ca}_{0.15}\text{NaNb}_5\text{O}_{15}$ ceramics prepared by the reactive templated grain growth, *Mater. Res. Bull.* **52**, 65 (2014).

- ⁸Y. Shi, X. Dong, F. Yan, K. Zhu, G. Ge, J. Lin, Y. Cao and J. Zhai, Rapid poling under low direct current field of [001] oriented BiFeO₃-based lead-free ceramics, *Scr. Mater.* **205**, 114181 (2021).
- ⁹W. Bai, D. Chen, P. Zheng, J. Zhang, B. Shen, J. Zhai and Z. Ji, Grain-orientated lead-free BNT-based piezoceramics with giant electrostrictive effect, *Ceram. Int.* **43**, 3339 (2017).
- ¹⁰L. Liu and Z. Hou, Fabrication of grain-oriented KSr₂Nb₅O₁₅ ceramics by a brush technique, *Mater. Lett.* **186**, 105 (2017).
- ¹¹S. Cao, Q. Chen, Y. Li, C. Wu, J. Xu, G. Cheng and F. Gao, Novel strategy for the enhancement of anti-counterfeiting ability of photochromic ceramics: Sm³⁺ doped KSr₂Nb₅O₁₅ textured ceramics with anisotropic luminescence modulation behavior, *J. Eur. Ceram. Soc.* **41**, 4924 (2021).
- ¹²Y. Zhang and L. Liu, Phase field simulation of abnormal grain growth mediated by initial particle size distribution, *Adv. Powder Technol.* **32**, 3395 (2021).
- ¹³L. Liu, X. Jiang, L. Rui, Z. Guo and Z. Hou, A duplex grain structure of dense (K, Na)NbO₃ ceramics constructed by using microcrystalline as seed, *J. Wuhan Univ. Technol.-Mat. Sci. Ed.* **37**, 385 (2022).
- ¹⁴P. R. Rios and M. E. Glicksman, Topological theory of abnormal grain growth, *Acta Mater.* **54**, 5313 (2006).
- ¹⁵L. Liu, Y. Wang, Y. Wang and R. Lv, Low-temperature dielectric anomalies in KSr₂Nb₅O₁₅ ceramics with tetragonal tungsten bronze structure: The effect of microstructure, *J. Alloys Compd.* **815**, 152397 (2020).
- ¹⁶Z. Shi, S. Cao, A. J. M. Araújo, P. Zhang, Z. Lou, M. Qin, J. Xu and F. Gao, Plate-like Ca₃Co₄O₉: A novel lead-free piezoelectric material, *Appl. Surf. Sci.* **536**, 147928 (2021).
- ¹⁷J. Xu, Y. Guo, K. Zhang, S. Liu, J. Zhao, E. Pawlikowska, M. Szafran and F. Gao, Monodisperse Ba_{0.6}Sr_{0.4}TiO₃ hollow spheres via a modified template-assisted method, *Appl. Surf. Sci.* **531**, 147315 (2020).
- ¹⁸R. Lv, L. Liu, Y. Wang and Y. Wang, A-site cation and morphology control of KSr₂Nb₅O₁₅ microcrystalline by a modified molten salt method, *Adv. Powder Technol.* **31**, 3256 (2020).
- ¹⁹L. Cheng and J. Li, A review on one dimensional perovskite nanocrystals for piezoelectric applications, *J. Materiomics* **2**, 25 (2016).
- ²⁰L. Liu, R. Lv, Z. Guo and Y. Wang, Fabrication of columnar NaNbO₃-based particles through topochemical microcrystal conversion, *Electron. Mater. Lett.* **16**, 55 (2020).
- ²¹S. K. Gupta and Y. Mao, A review on molten salt synthesis of metal oxide nanomaterials: Status, opportunity, and challenge, *Prog. Mater. Sci.* **117**, 100734 (2021).
- ²²Y. Zhang and L. Liu, Computational design of microstructures of textured ferroelectric ceramics by phase field simulation, *Comput. Mater. Sci.* **159**, 24 (2019).
- ²³L. Liu and Y. Zhang, Effect of initial particle size on grain microstructure of textured ferroelectric ceramics: A phase-field method and brush technique, *J. Eur. Ceram. Soc.* **42**, 5675 (2022).
- ²⁴L.-Q. Chen, Phase-field models for microstructure evolution, *Annu. Rev. Mater. Res.* **32**, 113 (2002).
- ²⁵D. Fan and L.-Q. Chen, Computer simulation of grain growth using a continuum field mode, *Acta Mater.* **45**, 611 (1997).
- ²⁶A. D. Moriana and S. J. Zhang, Determining the effects of BaTiO₃ template alignment on template grain growth of Pb(Mg_{1/3}Nb_{2/3})O₃-PbTiO₃ and effects on piezoelectric properties, *J. Eur. Ceram. Soc.* **42**, 2752 (2022).
- ²⁷W. Bai, L. Li, W. Li, B. Shen, J. Zhai and H. Chen, Effect of SrTiO₃ template on electric properties of textured BNT-BKT ceramics prepared by templated grain growth process, *J. Alloys Compd.* **603**, 149 (2014).
- ²⁸Q. Kou, B. Yang, Y. Sun, S. Yang, L. Liu, H. Xie, Y. Chang, S. Zhang and F. Li, Tetragonal (Ba, Ca)(Zr, Ti)O₃ textured ceramics with enhanced piezoelectric response and superior temperature stability, *J. Materiomics* **8**, 366 (2022).